

# All-to-key Attention for Arbitrary Style Transfer

Mingrui Zhu<sup>\*1</sup> Xiao He<sup>\*1</sup> Nannan Wang<sup>†1</sup> Xiaoyu Wang<sup>2</sup> Xinbo Gao<sup>3</sup>

<sup>\*</sup>equal technical contribution <sup>†</sup>corresponding author

<sup>1</sup>State Key Laboratory of Integrated Services Networks, Xidian University, Xi'an, China

<sup>2</sup>School of Computer Science and Technology, University of Science and Technology of China, Hefei, China

<sup>3</sup>Chongqing Key Laboratory of Image Cognition, Chongqing University of Posts and Telecommunications, Chongqing, China

## Abstract

Attention-based arbitrary style transfer studies have shown promising performance in synthesizing vivid local style details. They typically use the all-to-all attention mechanism: each position of content features is fully matched to all positions of style features. However, all-to-all attention tends to generate distorted style patterns and has quadratic complexity. It virtually limits both the effectiveness and efficiency of arbitrary style transfer. In this paper, we rethink what kind of attention mechanism is more appropriate for arbitrary style transfer. Our answer is a novel all-to-key attention mechanism: each position of content features is matched to key positions of style features. Specifically, it integrates two newly proposed attention forms: distributed and progressive attention. Distributed attention assigns attention to multiple key positions; Progressive attention pays attention from coarse to fine. All-to-key attention promotes the matching of diverse and reasonable style patterns and has linear complexity. The resultant module, dubbed StyA2K, has fine properties in rendering reasonable style textures and maintaining consistent local structure. Qualitative and quantitative experiments demonstrate that our method achieves superior results than state-of-the-art approaches.

## 1. Introduction

Arbitrary style transfer (AST) is an important computer vision task. It aims to render a natural image (known as content image) with the artistic style of an arbitrary painting (known as style image), enabling the generated image to imitate any artistic style. There have been notable improvements in feature transfer modules [6, 11, 12, 16, 26, 28, 31, 45, 46], novel architectures [1, 5, 23, 30, 39], and practical objectives [4, 18, 47]. The core of AST is the matching of content features and style features in the feed-forward procedure. Holistic feature distribution matching [12, 16, 23, 46] and locality-aware feature matching [11, 26, 28, 31, 45] are two

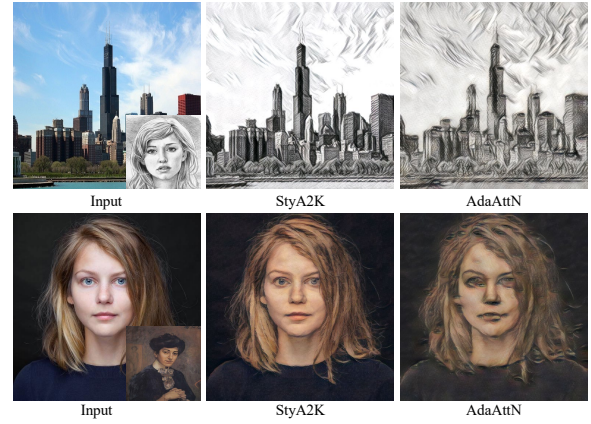


Figure 1. Style transfer results of AdaAttN [26] and our StyA2K. Massive unreasonable eye patterns distort the stylization results of AdaAttN. Our method can generate fine style details and maintain a consistent local structure.

categories of existing techniques.

The attention-based method is the research focus of the locality-aware feature matching category for its capability to capture long-range dependencies. Typically, it establishes a dense correspondence between point-wise tokens of the content and style features via an all-to-all attention mechanism [48]. The transferred feature of each local position is computed as the weighted sum of the local style features of all positions, where the weights are computed by applying a softmax function to the normalized dot products' results. Despite its encouraging results, the attention-based AST method suffers from two main predicaments. The first one is the introduction of distorted style patterns. For example, the stylization result of AdaAttN is seriously affected by eye patterns, which significantly affects the visual perception of the image, as shown in Figure 1. The second one is the high computational complexity.

We argue that the above problems are caused by the inherent limitations of the all-to-all attention mechanism. On the one hand, all-to-all attention has no error tolerance. It

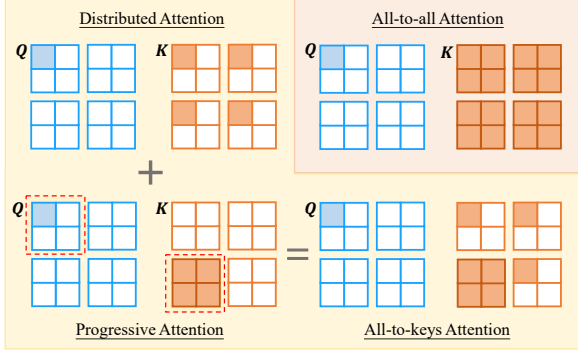


Figure 2. Illustration of the all-to-all attention mechanism and our proposed all-to-key attention mechanism. All-to-all attention matches all keys for each query. All-to-key attention matches partial keys for each query and integrates two kinds of attention forms (distributed attention and progressive attention).

prefers to assign a much larger weight to the value whose corresponding key is most similar to the query, given that softmax shows strong exclusiveness in attention score due to exponential computation. Therefore, all-to-all attention after softmax tends to concentrate on the most similar value. A distorted style pattern appears when the most similar key is semantically distinct from the query. For example, the reason for the appearance of irrational eye patterns in the results of AdaAttN is that the all-to-all attention operation almost exclusively concentrates on the eye patterns in the reference style image for the positions with edge-like patterns in the content image. On the other hand, all-to-all attention has quadratic computational complexity since it establishes a fully connected correspondence between queries and keys. Handling image features with high spatial resolution and dense elements exacerbates the issue that the computational complexity of the all-to-all attention operation scales quadratically with respect to image size.

The attention mechanism appropriate for AST should be capable of enhancing local style patterns via softmax but without introducing distorted style patterns due to its exclusivity. Our solution is a novel all-to-key attention (A2K) mechanism that matches each query with only “key” keys. It integrates two main characteristics. Firstly, keys are discretely and evenly distributed to different regions of the image rather than all positions, which helps to reduce the similar style patterns and accept more other style patterns. Hence, attention after softmax can distribute to several key locations rather than one. Secondly, attention is gradually focused from coarse-grained region to fine-grained key positions to match local style patterns from a more macro perspective. We name the former as distributed attention (DA) and the latter as progressive attention (PA). In this way, all-to-key attention mechanism can match multiple similar style patterns rather than the most one. promotes matching accurate local style patterns, as shown in Figure 1.

Technically, we implement DA and PA as two-axis blocked attention. The distributed attention axis conducts dilated attention to approximately distract the all-to-all attention. Regarding the progressive attention axis, we perform patch-wise attention in the first step to index coarse-grained regions and then conduct point-wise attention to locate the fine-grained positions. In this way, A2K establishes sparse correspondence with partial keys (local style features) for every query (local content feature), enjoying linear computational complexity, as shown in Figure 2. Besides, two novel objective functions are made possible by A2K. Finally, an effective and efficient arbitrary style transfer model based on **all-to-key** attention (StyA2K) arrives. We summarize the main contributions of this paper as the following points:

- We analyze the main problems that the attention-based method suffers and point out that the reason for these problems is the inherent limitations of the all-to-all attention mechanism.
- We present a novel all-to-key attention mechanism that integrates two newly proposed attention forms: distributed attention and progressive attention. All-to-key attention can synthesize accurate style patterns and enjoys linear computational complexity.
- Extensive experiments demonstrate the superiority of our method over state-of-the-art methods in rendering reasonable style textures and maintaining consistent structures.

## 2. Related Work

### 2.1. Arbitrary Style Transfer

Neural style transfer has become a hot-spot topic and has attracted wide attention since the pioneering work of Gatys *et al.* [9]. Follow-up studies [2, 8, 10, 15, 19, 20, 22, 24, 33, 34, 38] are devoted to improving the capabilities of neural style transfer algorithms in terms of visual quality, computational efficiency, style diversity, structural consistency, and factor controllability. Arbitrary style transfer [1, 3–6, 11, 12, 14, 16, 18, 21, 23, 26, 28, 31, 39, 41, 45–47] has received increasing attention recently, depending on its advantage of using a single feed-forward neural model to transfer the style of an arbitrary image. Existing AST methods can be divided into two main categories: holistic feature distribution matching method and locality-aware feature matching method.

The holistic feature distribution matching method adjusts the holistic content feature distribution to match the style feature distribution. Based on the Gaussian prior assumption, AdaIN [12] and WCT [23] match feature distributions with first- or second-order statistics. The method introduced in [21] makes the transformation matrix learnable. In order to break through the theoretical and practical limitations of

first-order and second-order statistics, high-order statistics are introduced in [16] and [46] to perform more exact distribution matching.

By comparison, the locality-aware feature matching method emphasizes the consistency of local semantics when matching content and style features. StyleSwap [3] replaces content features patch-by-patch with the style features, where the closest-matching style patches are calculated based on the normalized cross-correlation. The deep feature reshuffle module introduced in [11] reshuffles the style features according to the content features via a constrained normalized cross-correlation. Avatar-Net [31] decorates the content features with aligned style features obtained through a relaxed normalized cross-correlation. MST [45] employs clustering to divide style features into multi-modal style representations, which are matched with local content features via graph-based style matching. With the rise of self-attention [36], many studies [6, 26, 28, 41] apply it to AST. SANet [28] directly adopts attention-based feature matching for AST. AdaAttN [26] adopts attention scores to adaptively perform attentive normalization on the content features by calculating the per-point attention-weighted mean and variance of style features. However, these methods neglect the limitations of all-to-all attention and inevitably produce compromised results.

## 2.2. Attention Mechanism

Since being proposed, the attention mechanism has been widely used in the field of natural language processing (NLP) [36, 40] and computer vision [7, 37]. Extensive variants [27, 35, 42, 48] are introduced to improve its capability and computational efficiency. Many efforts [13, 28, 43] adapt spatial attention to match features with distinct distributions. In this work, we aim to explore an attention mechanism more appropriate for the AST task. Inspired by the multi-axis blocked self-attention proposed in [48], distributed attention and progressive attention in our proposed all-to-key attention mechanism are implemented as two-axis blocked attention with innovative modifications. Therefore they can be learned jointly and enjoy higher computing efficiency.

## 3. Method

### 3.1. Overall Architecture

An overview of our framework is presented in Figure 3. Given a content image  $I_c$  and a style image  $I_s$ , a pre-trained VGG-19 [32] network with fixed parameters is utilized as an encoder  $E_{nc}$  to extract their multi-scale features. Extracted features at each layer  $l$  can be denoted as:

$$F_c^l = E_{nc}(I_c), F_s^l = E_{nc}(I_s), \quad (1)$$

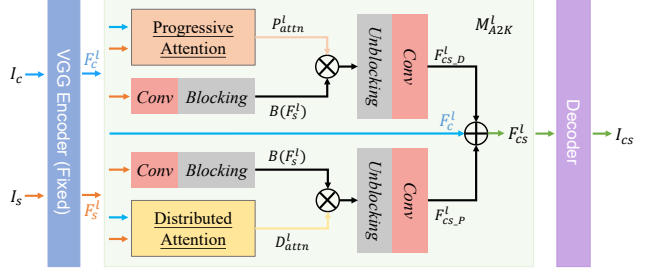


Figure 3. Overview of our framework.

where  $l \in \{ReLU\_3.1, ReLU\_4.1, ReLU\_5.1\}$ ,  $F_*^l \in \mathbb{R}^{C_l \times H_l \times W_l}$  and  $*$  can be  $c$  or  $s$  representing content and style respectively.

The key ingredient of this framework is the A2K module. It integrates two effective and efficient attention forms (distributed attention and progressive attention as illustrated in Figure 4) to establish meaningful sparse correspondence between the content feature  $F_c^l$  and the style feature  $F_s^l$  and thus faithfully synthesize the transferred features  $F_{cs}^l$ :

$$F_{cs}^l = M_{A2K}^l(F_c^l, F_s^l), \quad (2)$$

where  $M_{A2K}^l$  denotes the A2K module and  $l$  indicates that  $M_{A2K}^l$  operates independently on each layer of the multi-scale features.

Finally we can invert the multi-scale transferred features  $\{F_{cs}^l\}$  to synthesize the stylized image  $I_{cs}$  through a decoder  $D_{ec}$ :

$$I_{cs} = D_{ec}(\{F_{cs}^l\}). \quad (3)$$

The decoder implemented in this work follows the setting of [26], which mirrors the encoder and takes the multi-scale transferred features as input.

### 3.2. All-to-key Attention

**Revisit All-to-all Attention in AST.** Attention mechanism in AST is derived from self-attention [36] and is commonly used as a locality-aware feature matching method. Formally, given the content feature  $F_c^l$  and the style feature  $F_s^l$  with the size of  $(H^l, W^l, C^l)$  at layer  $l$ ,  $Q$  (query),  $K$  (key) and  $V$  (value) are formulated as:

$$Q = f(N(F_c^l)), K = g(N(F_s^l)), V = h(F_c^l), \quad (4)$$

where  $f$ ,  $g$ , and  $h$  are learnable convolution layers and  $N(*)$  denotes normalization operation. The attention score  $AttN$  can be calculated as:

$$AttN = softmax(Q \otimes K^T), \quad (5)$$

where  $\otimes$  denotes the dot product. The attention score  $AttN$ , with the size of  $(H \times W, H \times W)$ , is the dense similarity correspondence matrix of all the tokens in  $F_c^l$  and  $F_s^l$ . Since

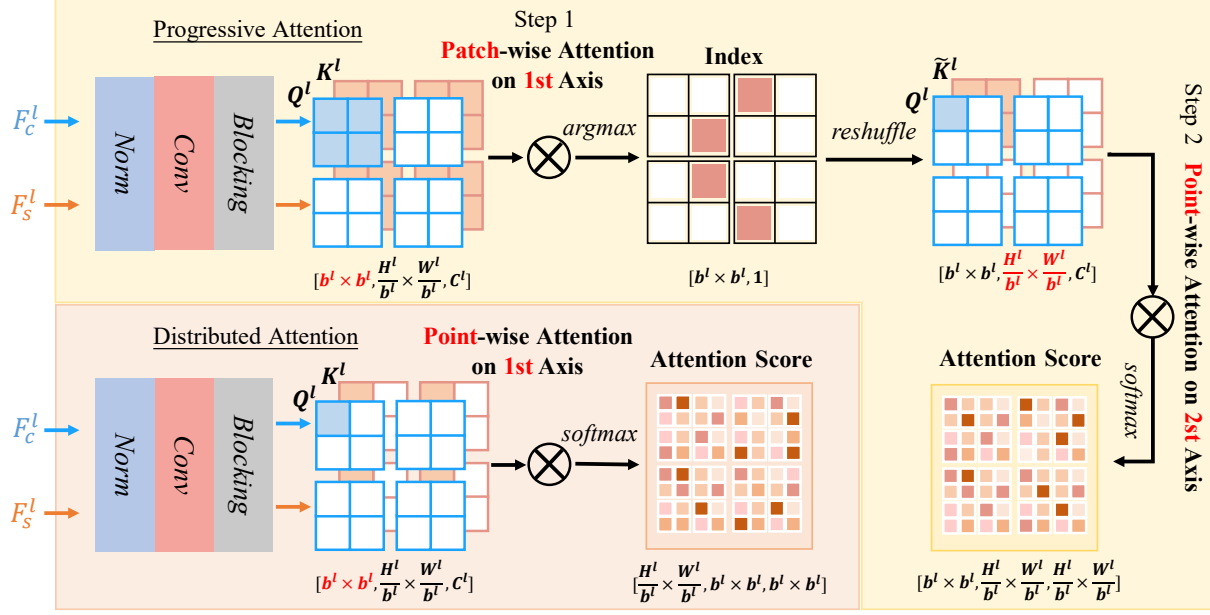


Figure 4. Distributed attention (DA) and progressive attention (PA) are implemented as two-axis blocked attention. DA calculates point-wise attention score along the first axis of  $Q^l$  and  $K^l$ . PA calculates patch-wise similarity index along the first axis of  $Q^l$  and  $K^l$  in the first step to reshuffle  $K^l$  to  $\tilde{K}^l$  and then calculates point-wise attention score on the second axis of  $Q^l$  and  $\tilde{K}^l$  in the second step.

this attention mechanism regards feature vectors of all spatial positions as tokens and establishes full correspondence (as shown in Figure 5 (b)), it is called all-to-all attention in [48]. Although all-to-all attention has been a key factor in many methods [26, 28, 41], its defects have not yet been found and studied. We argue that the all-to-all attention form is possibly inadequate for AST. As shown in Figure 5 (c), all-to-all attention after *softmax* concentrates almost all its attention on the eye pattern in the reference style image for the position with an edge-like pattern in the content image and thus inevitably contaminates this area with the matched eye pattern.

**Distributed Attention.** To alleviate the problem caused by all-to-all attention, distributed attention reduces the number of keys within the same local region so that attention is discretely and evenly *distributed* to different local regions of the image (as shown in Figure 5 (e)). This form of attention helps to assign higher weights to other style patterns that are not the most similar; thus, the attention after *softmax* (as shown in Figure 5 (f)) can concentrate on more positions and introduce more reasonable style patterns. Technically, we implement distributed attention as the form of dilated attention, which establishes a sparse correspondence between tokens with a fixed stride equal to the block size, as shown in Figure 4. To be specific, the content feature  $F_c^l$  and the style feature  $F_s^l$  with the size of  $(H^l, W^l, C^l)$  at each layer are spatially blocked into tensors that stand for  $Q^l$  and  $K^l$  respectively:

$$Q^l = B^l(N^l(F_c^l)), K^l = B^l(N^l(F_s^l)), \quad (6)$$

where  $N^l(*)$  denotes instance normalization and  $B^l(*)$  denotes  $1 \times 1$  Conv-Blocking operation. The shape of  $Q^l$  and  $K^l$  is  $(b^l \times b^l, \frac{H^l}{b^l} \times \frac{W^l}{b^l}, C^l)$ , representing  $b^l \times b^l$  non-overlapping blocks each with the size of  $(\frac{H^l}{b^l}, \frac{W^l}{b^l})$ . Distributed attention  $D^l$  calculates sparse attention score along the first axis of  $Q^l$  and  $K^l$ :

$$D_{attn}^l = D^l(Q^l, K^l). \quad (7)$$

The attention score matrix  $D_{attn}^l$ , with the size of  $(\frac{H^l}{b^l} \times \frac{W^l}{b^l}, b^l \times b^l, b^l \times b^l)$ , stores the sparse similarity correspondence of point-wise tokens across  $b^l \times b^l$  blocks and indexed in range  $\frac{H^l}{b^l} \times \frac{W^l}{b^l}$ . Note that attention along a specific axis of  $Q^l$  and  $K^l$  can be realized straightforwardly by einsum operation, which most deep learning frameworks have implemented. In addition, inspired by the multi-head attention in transformer [36], we use multiple heads to split the tensors along channel dimensions and project the divided tensors into different spaces for attention calculation.

**Progressive Attention.** All-to-all attention “cannot see the wood for the trees” since it focuses directly on a specific position. Progressive attention tackles this problem by *progressively* focusing from the coarse-grained region to the fine-grained position (as shown in Figure 5 (g) (h) (i)). Paying attention to the coarse-grained (as shown in Figure 5 (g)) in the first step contributes to matching style patterns on a larger scale; thus, the attention after *argmax* (as shown in Figure 5 (h)) can concentrate on a coarse style pattern with more similar semantics. Fine-grained positions



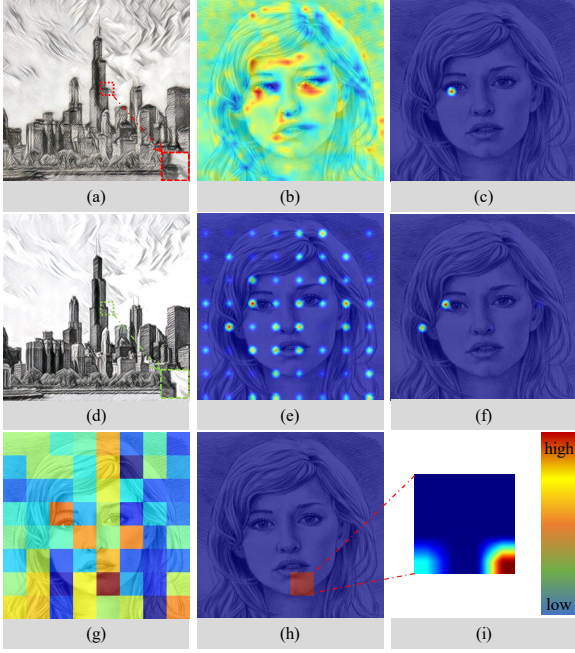


Figure 5. Visualization of attention distribution. (a) Stylized result of AdaAttN. (b) and (c) All-to-all attention distribution before and after softmax. (d) Stylized result of StyA2K. (e) and (f) Distributed attention distribution before and after softmax. (g) and (h) Progressive attention distribution on the coarse-grained region before and after argmax. (i) Progressive attention distribution on the fine-grained position after softmax.

can be further located via point-wise attention within this coarse-grained region. As shown in Figure 5 (i), progressive attention finally matches the chin edge, avoiding introducing an eye pattern. The technical implementation of progressive attention is shown in Figure 4.  $Q^l$  and  $K^l$  are obtained similarly as distributed attention but using a different  $1 \times 1$  Conv. The first step of progressive attention is implemented as patch-wise attention along the first axis, which takes a block region as a token instead of a specific position. Specifically, we use *argmax* to match only the most similar coarse-grained region, and therefore, the output of this step is the index matrix that stores sparse indices of patch-wise tokens across  $b^l \times b^l$  blocks:

$$P_{idx}^l = \text{argmax}(P_1^l(Q^l, K^l)), \quad (8)$$

where  $P_1^l$  denotes the first step of progressive attention. With  $P_{idx}^l$ , we can reshuffle the tokens of  $K^l$  and  $B(F_s^l)$  to semantically matching the spatial arrangement of the tokens of  $Q^l$ :

$$\begin{aligned} \tilde{K}^l &= \text{reshuffle}(K^l, P_{idx}^l), \\ \tilde{B}(F_s^l) &= \text{reshuffle}(B(F_s^l), P_{idx}^l), \end{aligned} \quad (9)$$

where  $\text{reshuffle}(*, *)$  denotes the reshuffle operation.

The second step of progressive attention  $P_2^l$  is implemented as regional attention, where tokens attend to their neighbors within non-overlapped blocks. Attention score in this step is calculated along the second axis of  $Q^l$  and  $\tilde{K}^l$ :

$$P_{attn}^l = P_2^l(Q^l, \tilde{K}^l). \quad (10)$$

The attention score matrix  $P_{attn}^l$ , with the size of  $(b^l \times b^l, \frac{H^l}{b^l} \times \frac{W^l}{b^l}, \frac{H^l}{b^l} \times \frac{W^l}{b^l})$ , stores the sparse similarity correspondence of point-wise tokens within blocks with the size of  $\frac{H^l}{b^l} \times \frac{W^l}{b^l}$  indexed in the range  $b^l \times b^l$ . Both steps of progressive attention can be implemented with einsum.

**Feature Transformation.** With the output attention score, the feature transformation of the two axes can be performed by:

$$\begin{aligned} F_{cs,D}^l &= U(D_{attn}^l \otimes B(F_s^l)), \\ F_{cs,P}^l &= U(P_{attn}^l \otimes \tilde{B}(F_s^l)), \end{aligned} \quad (11)$$

where  $U(*)$  denotes the Unblocking-Conv operation,  $\otimes$  represents the dot product between a specific axis of two tensors which can be implemented with einsum. The transferred feature at each layer  $l$  can be eventually obtained by:

$$F_{cs}^l = F_{cs,D}^l + F_{cs,P}^l + F_c^l, \quad (12)$$

where  $F_{cs,D}^l$ ,  $F_{cs,P}^l$  and  $F_c^l$  are the output of distributed attention axis, the output of progressive attention axis and content feature, respectively.

**Complexity Analysis.** The computational complexity of A2K is:

$$\begin{aligned} \Omega &= \Omega_D + \Omega_{P_1} + \Omega_{P_2} \\ &= (b)^2 HWC + (b)^2 HWC + \frac{H}{b} \frac{W}{b} HWC, \end{aligned} \quad (13)$$

which is linear with respect to image size  $HW$ , while all-to-all attention is quadratic.

### 3.3. Loss Function

The loss function for training the model consists of three terms. One of them is the style loss  $\mathcal{L}_{gs}$  followed by [12], which penalizes the Euclidean distances of mean  $\mu$  and standard deviation  $\sigma$  between stylized image and style image in VGG feature space to ensure global stylization effect:

$$\begin{aligned} \mathcal{L}_{gs} &= \sum_{l=1}^4 \|\mu(E_{nc}^l(I_{cs})) - \mu(F_s^l)\|_2 \\ &\quad + \sum_{l=1}^4 \|\sigma(E_{nc}^l(I_{cs})) - \sigma(F_s^l)\|_2, \end{aligned} \quad (14)$$

where  $E_{nc}^l(*)$  denotes feature extracted from the  $l$ th layer of the pre-trained VGG encoder. The second term is a novel

attention-based feature matching loss that penalizes the Euclidean distance between the transferred features of A2K module and the features of the stylized image:

$$\mathcal{L}_{A2K^*} = \sum_{l=2}^5 \|E_{nc}^l(I_{cs}) - M_{A2K^*}^l(F_c^l, F_s^l)\|_2, \quad (15)$$

where  $M_{A2K^*}^l$  denotes a non-parametric version that removes the learnable  $1 \times 1$  Conv because the supervision signal should be deterministic. The third loss term is a mixed version of A2K and AdaAttN. We directly replace the all-to-all attention used in AdaAttN with our A2K module to obtain a power-enhanced AdaA2K module. The new attention-based feature matching loss can be formulated as follows:

$$\mathcal{L}_{AdaA2K^*} = \sum_{l=2}^5 \|E_{nc}^l(I_{cs}) - M_{AdaA2K^*}^l(F_c^l, F_s^l)\|_2, \quad (16)$$

where  $M_{AdaA2K^*}^l$  is also a parametric-free version of AdaA2K module. The full loss can be calculated by:

$$\mathcal{L} = \lambda_1 \mathcal{L}_{gs} + \lambda_2 \mathcal{L}_{A2K^*} + \lambda_3 \mathcal{L}_{AdaA2K^*}. \quad (17)$$

## 4. Experiments

### 4.1. Implementing Details

We use images from MS-COCO [25] as content and images from WikiArt [29] as style to train our model.  $\lambda_1$ ,  $\lambda_2$ , and  $\lambda_3$  in Eq. 17 are set as 10, 0.5, and 1.5, respectively. The batch size is set to 8, and the training lasts for five epochs (400K iterations) on a single NVIDIA GeForce RTX 3090 GPU. Adam [17] with momentum parameters  $\beta_1 = 0.9$  and  $\beta_2 = 0.999$  is used for optimization. The learning rate is set to  $2e-4$  for the first two epochs and linearly decayed to 0 for the rest three epochs. Images are randomly cropped to  $256 \times 256$  during training and loaded with  $512 \times 512$  while inference. To ensure that DA and PA are computed on input sequences of similar length, the tensors need to be blocked in a balanced way such that  $b^l \times b^l \approx \frac{H^l}{b^l} \times \frac{W^l}{b^l}$ . Therefore the block size  $b$  is set to 16, 8, 8, and 4 for *ReLU\_2.1*, *ReLU\_3.1*, *ReLU\_4.1* and *ReLU\_5.1* layers, respectively. The number of heads is set to 8.

### 4.2. Comparison with Prior Arts

To validate the effectiveness of the proposed method, we compare it with six previous state-of-the-art AST methods: StyTr<sup>2</sup> [5], AdaAttN [26], SANet [28], MST [45], Avatar-Net [31], and AdaIN [12]. We obtain the results of the comparison methods by running their official code with the default configuration.

**Qualitative Comparisons.** We show the visual comparisons between our model and other AST methods in Figure 5. Adam adjusts the holistic feature distribution and

has no local content awareness; therefore, its results can only roughly transfer the holistic style. Avatar-Net utilizes a relaxed normalized cross-correlation to fulfill locality-aware feature matching so that its results partially maintain semantic consistency. The results are significantly distorted, though, because it only matches the most similar style pattern. MST clusters the complex style distribution into sub-style components and manipulates the features by graph-based patch matching. Despite its promising results, distorted structures still exist. Additionally, it heavily relies on the effect of clustering. SANet adopts an attention mechanism to match style features for local content features attentively. AdaAttN combines attention mechanism and adaptive instance normalization to integrate the advantage of locality-aware feature matching and holistic feature matching. Their results show a consistent structure and fine local style details. However, due to the limitation of all-to-all attention, their results contain many unreasonable style patterns (2nd, 3rd, and 5th row). StyTr<sup>2</sup> adapts transformer architecture to AST and achieves cutting-edge performance. Their results still suffer from unreasonable textures (2rd, 4td, and 6th row). Our proposed StyA2K outperforms other methods in visual quality, maintaining more consistent structures and generating detailed local style textures without introducing many unappealing artifacts.

**Quantitative Comparisons.** Following [5], we compute the average content loss between the generated results and input content images and the average style loss between the generated results and input style images to measure how well the input content and style are preserved. The smaller the value is, the better the input content/style is preserved. In addition, we adopt the Learned Perceptual Image Patch Similarity (LPIPS) [44] metric to calculate the quality difference between the generated and input content images. A lower score indirectly indicates better quality of generated images. We randomly select 15 content images and 20 style images to generate 300 stylized images. Table 1 shows the corresponding quantitative results. Our proposed model outperforms state-of-the-art methods on all three evaluation metrics.

**User Study.** We conduct a user study to evaluate human preference on the results generated by different methods. We reuse the images in the quantitative comparisons and randomly sample 20 groups. Each group consists of a content image, a style image, and seven stylized images generated by different methods. The order of stylized images in each group is shuffled. We ask participants to select their favorite stylized image in each group from three perspectives: content preservation, stylization effect, and overall preference. We collect 1600 votes for each view from 80 participants. Table 1 shows the statistics of the votes, which indicate that the results generated by our method are more appealing than other methods.

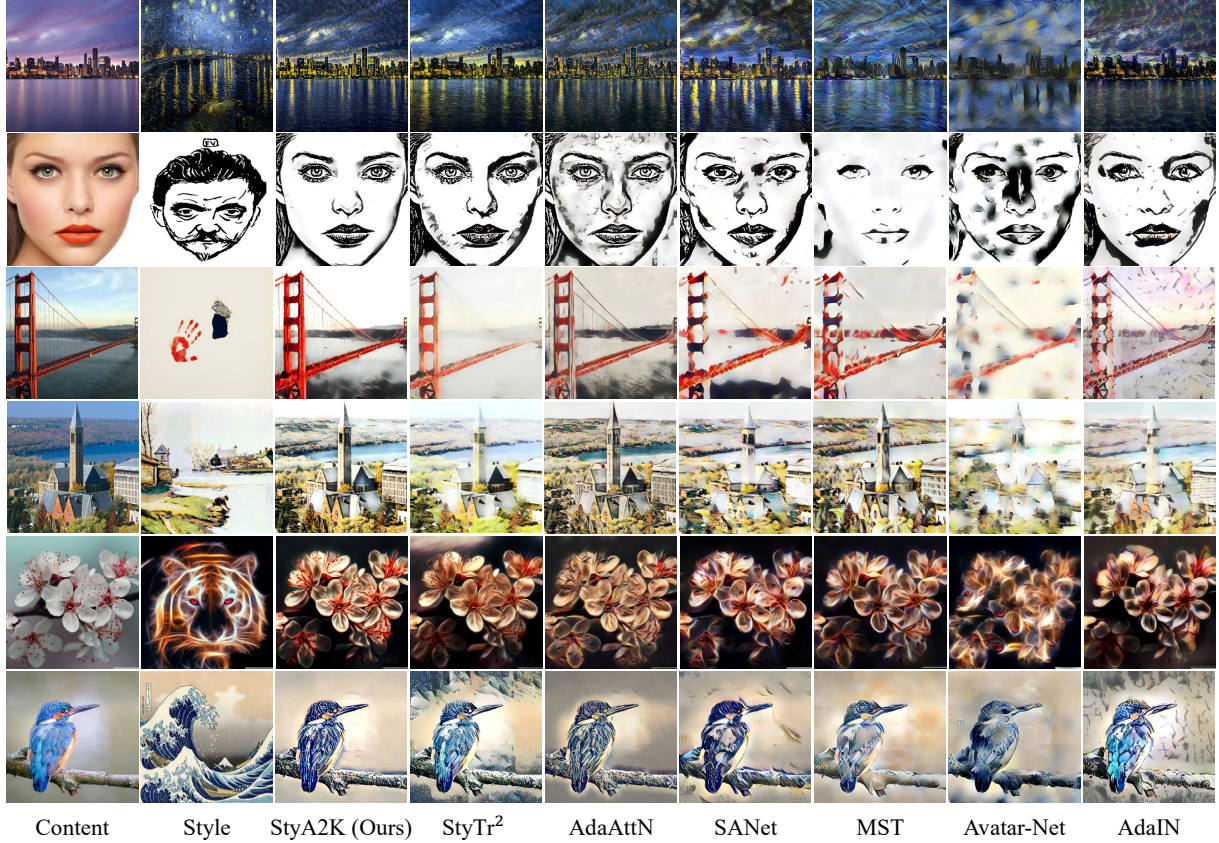


Figure 6. Visual comparisons among different AST methods. Zoom in for a better view.

Table 1. Statics of quantitative comparison, user study, and inference time. The best results are in **bold** and the second best results are marked with an underline.

Method		StyA2K (Ours)	StyTr <sup>2</sup>	AdaAttN	SANet	MST	Avatar-Net	AdaIN
Evaluation Metrics	Content Loss ↓	<b>0.74</b>	0.83	1.00	0.96	<u>0.77</u>	1.26	0.91
	Style Loss ↓	<b>0.96</b>	1.20	1.24	<u>0.99</u>	2.65	3.96	1.16
	LPIPS ↓	<b>0.56</b>	0.57	0.59	0.63	<u>0.57</u>	0.64	0.62
User Study	Content Per. ↑	<b>52.69</b>	9.81	<u>15.56</u>	7.12	8.19	2.25	4.38
	Style Per. ↑	<b>29.06</b>	14.81	12.38	<u>16.13</u>	11.31	9.13	7.19
	Overall Per. ↑	<b>36.06</b>	<u>15.81</u>	14.50	11.44	11.63	3.56	7.00
Inference Time (Sec./Image) ↓		0.0121	0.1004	0.0269	<u>0.0041</u>	1.3906	0.3348	<b>0.0038</b>

**Efficiency Comparison.** We report the average inference time of StyA2K and other AST methods under  $512 \times 512$  resolution in Table 1. StyA2K achieves 80 FPS at  $512 \times 512$  resolution, which can generate stylized images in real-time. StyA2K is superior to AdaAttN and comparable with SANet, which uses only two feature layers.

### 4.3. Ablation Study

We conduct an ablation study to verify the effectiveness of the key ingredients in our method. Visual and quantitative results are shown in Figure 7 and Table 2, respectively.

**Effect of All-to-key Attention.** To demonstrate the superiority of our proposed all-to-key attention over all-to-all attention, we replace the all-to-key attention in our full model with all-to-all attention and observe the changes in visual quality and evaluation scores. As shown in Figure 7, the model using all-to-all attention produces distorted style patterns in its result. The evaluation scores in Table 2 increase slightly. The results suggest that all-to-key attention alleviates the defects caused by all-to-all attention.

**Effect of DA and PA.** To validate the respective effectiveness of DA and PA, we set up three variants: 1) full



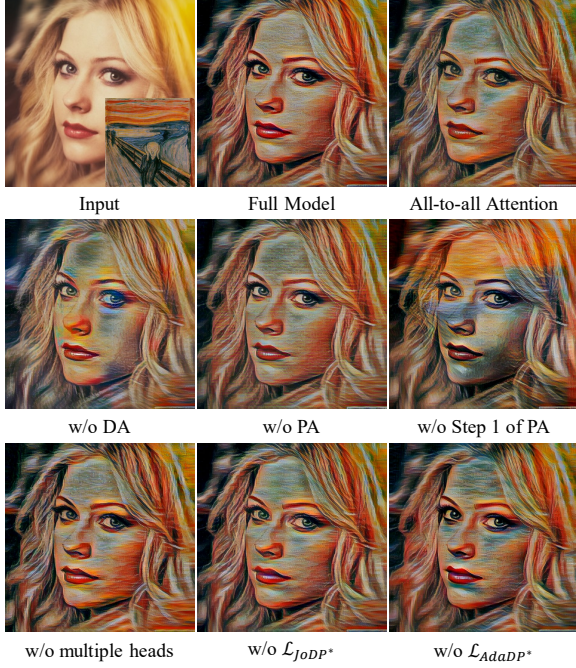


Figure 7. Ablation study on the key ingredients of the proposed method. Zoom-in for a better view.

model without DA, 2) full model without PA, and 3) full model without the first step of PA. As shown in Figure 7, the model without DA assigns too much attention to local style patterns and loses structural consistency in its result. The model without PA tends to lose fine color and texture details in its result. When removing the first step, PA directly performs regional attention within local blocks; therefore, its result is mixed with the spatially copied style patterns, which deviates from our original intention. This is also why the variant has the minimum average style loss, as shown in Table 2. In addition, the average content loss and the average LPIPS score increase when removing one of the three components. Therefore, we can conclude that all three ingredients are critical to the final effect of the model.

**Effect of  $\mathcal{L}_{A2K^*}$  and  $\mathcal{L}_{AdaA2K^*}$ .** We train our model without  $\mathcal{L}_{A2K^*}$  and  $\mathcal{L}_{AdaA2K^*}$ , respectively, to verify the effectiveness of each loss term. The visual quality drops significantly when training the model without each loss term, as shown in Figure 7. This indicates that both  $\mathcal{L}_{A2K^*}$  and  $\mathcal{L}_{AdaA2K^*}$  are critical to the final effect of the model.

**Effect of Multiple Heads.** The removal of multiple heads (i.e., using only one head) leads to slight visual quality degradation and loss increase, as shown in Figure 7 and Table 2. We can conclude that multiple heads help to improve the effect.

#### 4.4. Multi-style Transfer

Following previous studies [6, 26, 28], StyA2K can achieve style interpolation between different styles and ac-

Table 2. Ablation study on the key ingredients of the proposed method. The best results are in **bold** and the second best results are marked with an underline.

Model	Content Loss ↓	Style Loss ↓	LPIPS ↓
All-to-all Attention	0.75	0.97	<u>0.56</u>
w/o DA	0.88	1.24	0.57
w/o PA	0.78	0.82	0.59
w/o Step 1 of PA	0.95	<b>0.47</b>	0.62
w/o $\mathcal{L}_{A2K^*}$	0.85	0.92	0.59
w/o $\mathcal{L}_{AdaA2K^*}$	<u>0.75</u>	<u>0.74</u>	0.59
w/o multiple heads	0.85	1.04	0.58
Full Model	<b>0.74</b>	0.96	<b>0.56</b>

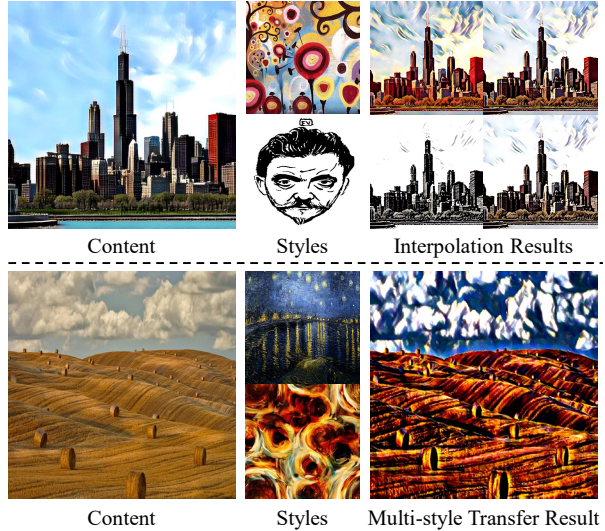


Figure 8. Results of style interpolation and multi-style transfer.

complish multi-style transfer that integrates multiple styles in one output image, as shown in Figure 8. These results demonstrate the flexibility of StyA2K.

## 5. Conclusion and Limitation

This paper proposes a novel all-to-key attention mechanism to achieve effective and efficient arbitrary style transfer. It integrates two newly proposed attention forms: distributed attention and progressive attention. Distributed attention divides attention across several key positions, while progressive attention concentrates attention from coarse to fine. Further, it facilitates two powerful objective functions to boost the model’s training. Our method achieves state-of-the-art results both quantitatively and qualitatively.

**Limitation.** The major limitation in this study is that the tensors need to be blocked in a balanced way to ensure that DA and PA are computed on input sequences of similar length; otherwise, the effect of the model will be affected. We will explore a more reasonable manner to divide blocks in our future work.



## References

- [1] Jie An, Siyu Huang, Yibing Song, Dejing Dou, Wei Liu, and Jiebo Luo. Artflow: Unbiased image style transfer via reversible neural flows. In *Proceedings of the IEEE/CVF Conference on Computer Vision and Pattern Recognition*, pages 862–871, 2021. 1, 2
- [2] Dongdong Chen, Lu Yuan, Jing Liao, Nenghai Yu, and Gang Hua. Stylebank: An explicit representation for neural image style transfer. In *Proceedings of the IEEE conference on computer vision and pattern recognition*, pages 1897–1906, 2017. 2
- [3] Tian Qi Chen and Mark Schmidt. Fast patch-based style transfer of arbitrary style. *arXiv preprint arXiv:1612.04337*, 2016. 2, 3
- [4] Jiaxin Cheng, Ayush Jaiswal, Yue Wu, Pradeep Natarajan, and Prem Natarajan. Style-aware normalized loss for improving arbitrary style transfer. In *Proceedings of the IEEE/CVF Conference on Computer Vision and Pattern Recognition*, pages 134–143, 2021. 1, 2
- [5] Yingying Deng, Fan Tang, Weiming Dong, Chongyang Ma, Xingjia Pan, Lei Wang, and Changsheng Xu. Stytr2: Image style transfer with transformers. In *Proceedings of the IEEE/CVF Conference on Computer Vision and Pattern Recognition*, pages 11326–11336, 2022. 1, 2, 6
- [6] Yingying Deng, Fan Tang, Weiming Dong, Wen Sun, Feiyue Huang, and Changsheng Xu. Arbitrary style transfer via multi-adaptation network. In *Proceedings of the 28th ACM international conference on multimedia*, pages 2719–2727, 2020. 1, 2, 3, 8
- [7] Alexey Dosovitskiy, Lucas Beyer, Alexander Kolesnikov, Dirk Weissenborn, Xiaohua Zhai, Thomas Unterthiner, Mostafa Dehghani, Matthias Minderer, Georg Heigold, Sylvain Gelly, et al. An image is worth 16x16 words: Transformers for image recognition at scale. *arXiv preprint arXiv:2010.11929*, 2020. 3
- [8] Vincent Dumoulin, Jonathon Shlens, and Manjunath Kudlur. A learned representation for artistic style. *arXiv preprint arXiv:1610.07629*, 2016. 2
- [9] Leon A Gatys, Alexander S Ecker, and Matthias Bethge. Image style transfer using convolutional neural networks. In *Proceedings of the IEEE conference on computer vision and pattern recognition*, pages 2414–2423, 2016. 2
- [10] Leon A Gatys, Alexander S Ecker, Matthias Bethge, Aaron Hertzmann, and Eli Shechtman. Controlling perceptual factors in neural style transfer. In *Proceedings of the IEEE conference on computer vision and pattern recognition*, pages 3985–3993, 2017. 2
- [11] Shuyang Gu, Congliang Chen, Jing Liao, and Lu Yuan. Arbitrary style transfer with deep feature reshuffle. In *Proceedings of the IEEE Conference on Computer Vision and Pattern Recognition*, pages 8222–8231, 2018. 1, 2, 3
- [12] Xun Huang and Serge Belongie. Arbitrary style transfer in real-time with adaptive instance normalization. In *Proceedings of the IEEE international conference on computer vision*, pages 1501–1510, 2017. 1, 2, 5, 6
- [13] Wentao Jiang, Si Liu, Chen Gao, Jie Cao, Ran He, Jiashi Feng, and Shuicheng Yan. Psgan: Pose and expression robust spatial-aware gan for customizable makeup transfer. In *Proceedings of the IEEE/CVF Conference on Computer Vision and Pattern Recognition*, pages 5194–5202, 2020. 3
- [14] Yongcheng Jing, Xiao Liu, Yukang Ding, Xinchao Wang, Errui Ding, Mingli Song, and Shilei Wen. Dynamic instance normalization for arbitrary style transfer. In *Proceedings of the AAAI Conference on Artificial Intelligence*, volume 34, pages 4369–4376, 2020. 2
- [15] Justin Johnson, Alexandre Alahi, and Li Fei-Fei. Perceptual losses for real-time style transfer and super-resolution. In *European conference on computer vision*, pages 694–711. Springer, 2016. 2
- [16] Nikolai Kalischek, Jan D Wegner, and Konrad Schindler. In the light of feature distributions: moment matching for neural style transfer. In *Proceedings of the IEEE/CVF Conference on Computer Vision and Pattern Recognition*, pages 9382–9391, 2021. 1, 2, 3
- [17] Diederik P Kingma and Jimmy Ba. Adam: A method for stochastic optimization. *arXiv preprint arXiv:1412.6980*, 2014. 6
- [18] Dmytro Kotovenko, Artsiom Sanakoyeu, Sabine Lang, and Bjorn Ommer. Content and style disentanglement for artistic style transfer. In *Proceedings of the IEEE/CVF international conference on computer vision*, pages 4422–4431, 2019. 1, 2
- [19] Chuan Li and Michael Wand. Combining markov random fields and convolutional neural networks for image synthesis. In *Proceedings of the IEEE conference on computer vision and pattern recognition*, pages 2479–2486, 2016. 2
- [20] Chuan Li and Michael Wand. Precomputed real-time texture synthesis with markovian generative adversarial networks. In *European conference on computer vision*, pages 702–716. Springer, 2016. 2
- [21] Xueting Li, Sifei Liu, Jan Kautz, and Ming-Hsuan Yang. Learning linear transformations for fast image and video style transfer. In *Proceedings of the IEEE/CVF Conference on Computer Vision and Pattern Recognition*, pages 3809–3817, 2019. 2
- [22] Yijun Li, Chen Fang, Jimei Yang, Zhaowen Wang, Xin Lu, and Ming-Hsuan Yang. Diversified texture synthesis with feed-forward networks. In *Proceedings of the IEEE conference on computer vision and pattern recognition*, pages 3920–3928, 2017. 2
- [23] Yijun Li, Chen Fang, Jimei Yang, Zhaowen Wang, Xin Lu, and Ming-Hsuan Yang. Universal style transfer via feature transforms. *Advances in neural information processing systems*, 30, 2017. 1, 2
- [24] Jing Liao, Yuan Yao, Lu Yuan, Gang Hua, and Sing Bing Kang. Visual attribute transfer through deep image analogy. *arXiv preprint arXiv:1705.01088*, 2017. 2
- [25] Tsung-Yi Lin, Michael Maire, Serge Belongie, James Hays, Pietro Perona, Deva Ramanan, Piotr Dollár, and C Lawrence Zitnick. Microsoft coco: Common objects in context. In *ECCV*, pages 740–755. Springer, 2014. 6
- [26] Songhua Liu, Tianwei Lin, Dongliang He, Fu Li, Meiling Wang, Xin Li, Zhengxing Sun, Qian Li, and Errui Ding. Adaattn: Revisit attention mechanism in arbitrary neural

- style transfer. In *Proceedings of the IEEE/CVF international conference on computer vision*, pages 6649–6658, 2021. 1, 2, 3, 4, 6, 8, 11
- [27] Ze Liu, Yutong Lin, Yue Cao, Han Hu, Yixuan Wei, Zheng Zhang, Stephen Lin, and Baining Guo. Swin transformer: Hierarchical vision transformer using shifted windows. In *Proceedings of the IEEE/CVF International Conference on Computer Vision*, pages 10012–10022, 2021. 3
- [28] Dae Young Park and Kwang Hee Lee. Arbitrary style transfer with style-attentional networks. In *proceedings of the IEEE/CVF conference on computer vision and pattern recognition*, pages 5880–5888, 2019. 1, 2, 3, 4, 6, 8
- [29] Fred Phillips and Brandy Mackintosh. Wiki art gallery, inc.: A case for critical thinking. *Issues in Accounting Education*, 26(3):593–608, 2011. 6
- [30] Falong Shen, Shuicheng Yan, and Gang Zeng. Neural style transfer via meta networks. In *Proceedings of the IEEE Conference on Computer Vision and Pattern Recognition*, pages 8061–8069, 2018. 1
- [31] Lu Sheng, Ziyi Lin, Jing Shao, and Xiaogang Wang. Avatar-net: Multi-scale zero-shot style transfer by feature decoration. In *Proceedings of the IEEE conference on computer vision and pattern recognition*, pages 8242–8250, 2018. 1, 2, 3, 6
- [32] Karen Simonyan and Andrew Zisserman. Very deep convolutional networks for large-scale image recognition. *arXiv preprint arXiv:1409.1556*, 2014. 3
- [33] Dmitry Ulyanov, Vadim Lebedev, Andrea Vedaldi, and Victor S Lempitsky. Texture networks: Feed-forward synthesis of textures and stylized images. In *International Conference on Machine Learning*, volume 1, page 4, 2016. 2
- [34] Dmitry Ulyanov, Andrea Vedaldi, and Victor Lempitsky. Improved texture networks: Maximizing quality and diversity in feed-forward stylization and texture synthesis. In *Proceedings of the IEEE conference on computer vision and pattern recognition*, pages 6924–6932, 2017. 2
- [35] Ashish Vaswani, Prajit Ramachandran, Aravind Srinivas, Niki Parmar, Blake Hechtman, and Jonathon Shlens. Scaling local self-attention for parameter efficient visual backbones. In *Proceedings of the IEEE/CVF Conference on Computer Vision and Pattern Recognition*, pages 12894–12904, 2021. 3
- [36] Ashish Vaswani, Noam Shazeer, Niki Parmar, Jakob Uszkoreit, Llion Jones, Aidan N Gomez, Łukasz Kaiser, and Illia Polosukhin. Attention is all you need. *Advances in neural information processing systems*, 30, 2017. 3, 4
- [37] Xiaolong Wang, Ross Girshick, Abhinav Gupta, and Kaiming He. Non-local neural networks. In *Proceedings of the IEEE conference on computer vision and pattern recognition*, pages 7794–7803, 2018. 3
- [38] Xin Wang, Geoffrey Oxholm, Da Zhang, and Yuan-Fang Wang. Multimodal transfer: A hierarchical deep convolutional neural network for fast artistic style transfer. In *Proceedings of the IEEE conference on computer vision and pattern recognition*, pages 5239–5247, 2017. 2
- [39] Xiaolei Wu, Zhihao Hu, Lu Sheng, and Dong Xu. Style-former: Real-time arbitrary style transfer via parametric style composition. In *Proceedings of the IEEE/CVF International Conference on Computer Vision*, pages 14618–14627, 2021. 1, 2
- [40] Zhilin Yang, Zihang Dai, Yiming Yang, Jaime Carbonell, Russ R Salakhutdinov, and Quoc V Le. Xlnet: Generalized autoregressive pretraining for language understanding. *Advances in neural information processing systems*, 32, 2019. 3
- [41] Yuan Yao, Jianqiang Ren, Xuansong Xie, Weidong Liu, Yong-Jin Liu, and Jun Wang. Attention-aware multi-stroke style transfer. In *Proceedings of the IEEE/CVF Conference on Computer Vision and Pattern Recognition*, pages 1467–1475, 2019. 2, 3, 4
- [42] Tan Yu, Gangming Zhao, Ping Li, and Yizhou Yu. Boat: Bilateral local attention vision transformer. *arXiv preprint arXiv:2201.13027*, 2022. 3
- [43] Pan Zhang, Bo Zhang, Dong Chen, Lu Yuan, and Fang Wen. Cross-domain correspondence learning for exemplar-based image translation. In *Proceedings of the IEEE/CVF Conference on Computer Vision and Pattern Recognition*, pages 5143–5153, 2020. 3
- [44] Richard Zhang, Phillip Isola, Alexei A Efros, Eli Shechtman, and Oliver Wang. The unreasonable effectiveness of deep features as a perceptual metric. In *Proceedings of the IEEE conference on computer vision and pattern recognition*, pages 586–595, 2018. 6
- [45] Yulun Zhang, Chen Fang, Yilin Wang, Zhaowen Wang, Zhe Lin, Yun Fu, and Jimei Yang. Multimodal style transfer via graph cuts. In *Proceedings of the IEEE/CVF International Conference on Computer Vision*, pages 5943–5951, 2019. 1, 2, 3, 6
- [46] Yabin Zhang, Minghan Li, Ruihuang Li, Kui Jia, and Lei Zhang. Exact feature distribution matching for arbitrary style transfer and domain generalization. In *Proceedings of the IEEE/CVF Conference on Computer Vision and Pattern Recognition*, pages 8035–8045, 2022. 1, 2, 3
- [47] Yuxin Zhang, Fan Tang, Weiming Dong, Haibin Huang, Chongyang Ma, Tong-Yee Lee, and Changsheng Xu. Domain enhanced arbitrary image style transfer via contrastive learning. In *ACM SIGGRAPH 2022 Conference Proceedings*, pages 1–8, 2022. 1, 2
- [48] Long Zhao, Zizhao Zhang, Ting Chen, Dimitris Metaxas, and Han Zhang. Improved transformer for high-resolution gans. *Advances in Neural Information Processing Systems*, 34:18367–18380, 2021. 1, 3, 4

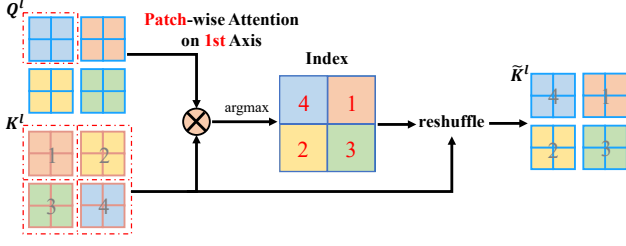


Figure 9. Detailed illustration of the step 1 in PA.

## A. Implementation Details

### A.1. Code

We provide the full code of our proposed StyA2K model. Please refer to the "README.md" file located in the Code folder for detailed usage of the code.

### A.2. Step 1 of PA

Figure 9 gives a more detailed illustration of the first step in progressive attention. The first step of progressive attention is implemented as patch-wise attention along the first axis, which takes a block region as a token instead of a specific position. In this step, we apply  $\text{argmax}$  to the attention score to obtain the indices of the most similar coarse-grained region. For example, the 4th block region in  $K^l$  is matched as the coarse-grained region most similar to the blue block region in  $Q^l$ , so the index of this region is set to 4. With the indices, we can reshuffle the tokens of  $K^l$  to semantically match the spatial arrangement of the tokens of  $Q^l$ . The reshuffled  $\tilde{K}^l$  is further utilized in the second step of PA.

### A.3. Decoder Architecture

The decoder implemented in this work follows the setting of [26], which mirrors the encoder and takes the multi-scale transferred features as input. Full decoder configuration is shown in Table 3. The decoder takes the multi-scale transferred features  $F_{cs}^l$  as input and gradually synthesizes the final image  $I_{cs}$ .

### A.4. All-to-key Attention Algorithm

The PyTorch code for our proposed all-to-key attention mechanism is shown in Algorithm 1. The implementation is elegant with the usage of einsum notation.

### A.5. Blocking and Unblocking Algorithm

The PyTorch code for feature blocking and unblocking operation in the all-to-key attention mechanism is shown in Algorithm 2

Table 3. Full configuration of the decoder.

Stage	Output	Architecture
$F^5$	$512 \times \frac{H}{8} \times \frac{W}{8}$	Input $F_{cs}^5$ Upsample scale 2 Add $F_{cs}^4$ $3 \times 3$ Conv, 512, ReLU
$F^4$	$256 \times \frac{H}{4} \times \frac{W}{4}$	$3 \times 3$ Conv, 256, ReLU Upsample scale 2
$F^3$	$128 \times \frac{H}{2} \times \frac{W}{2}$	Concatenate $F_{cs}^3$ $(3 \times 3 \text{ Conv}, 256, \text{ReLU}) \times 3$ $3 \times 3$ Conv, 128, ReLU Upsample scale 2
$F^2$	$64 \times H \times W$	$3 \times 3$ Conv, 128, ReLU $3 \times 3$ Conv, 64, ReLU Upsample scale 2
$F^1$	$3 \times H \times W$	$3 \times 3$ Conv, 64, ReLU $3 \times 3$ Conv, 3

### A.6. Loss Function

**Details of  $\mathcal{L}_{AdaA2K^*}$ .** The third loss term used to train StyA2K is a mixed version of the A2K and AdaAttN modules. AdaAttN proposed in [26] provides an effective way to combine the advantage of locality-aware feature matching and holistic feature matching. It calculates attention-weighted mean  $M^l$  and attention-weighted standard variance  $S^l$  based on the all-to-all attention mechanism to adjust the holistic content feature distribution:

$$\begin{aligned}
 M^l &= F_s^l \otimes \text{AttN}^T, \\
 S^l &= \sqrt{(F_s^l \cdot F_s^l) \otimes \text{AttN}^T - M \cdot M}, \\
 F_{cs}^l &= S^l \cdot \text{Norm}(F_c^l) + M^l,
 \end{aligned} \tag{18}$$

where  $l \in \{\text{ReLU}_{2.1}, \text{ReLU}_{3.1}, \text{ReLU}_{4.1}, \text{ReLU}_{5.1}\}$  and  $\text{AttN}$  denotes the attention score calculated by the all-to-all attention. Following this idea, we replace the all-to-all attention used in AdaAttN with our all-to-key attention to obtain a power-enhanced AdaA2K module. More specifically, the attention-weighted mean and attention-weighted standard variance calculated by distributed attention and progressive attention are added together to adjust the holistic content feature distribution jointly:

$$\begin{aligned}
 M_d^l &= U(B(F_s^l) \otimes D_{attn}^l), \\
 S_d^l &= \sqrt{U((B(F_s^l) \cdot B(F_s^l)) \otimes D_{attn}^l) - M_d^l \cdot M_d^l}, \\
 M_p^l &= U(B(F_s^l) \otimes P_{attn}^l), \\
 S_p^l &= \sqrt{U((B(F_s^l) \cdot B(F_s^l)) \otimes P_{attn}^l) - M_p^l \cdot M_p^l}, \\
 F_{cs}^l &= (S_d^l + S_p^l) \cdot \text{Norm}(F_c^l) + (M_d^l + M_p^l),
 \end{aligned} \tag{19}$$

where  $B(*)$  denotes the blocking operation,  $U(*)$  denotes the unblocking operation,  $D_{attn}^l$  is the attention score calcu-

Table 4. Evaluation scores of the results generated under different ratios. The best results are in **bold**.

$\lambda_3 / (\lambda_2 + \lambda_3)$	Content Loss ↓	Style Loss ↓	LPIPS ↓
0	<b>0.53</b>	1.14	<b>0.52</b>
0.25	0.59	1.09	0.53
0.5	0.65	0.98	0.55
0.75	0.74	<b>0.96</b>	0.56
1	0.83	0.97	0.58

lated by the distributed attention, and  $P_{attn}^l$  is the attention score calculated by the progressive attention.

**Setting of  $\lambda_1$ ,  $\lambda_2$ , and  $\lambda_3$ .** We empirically set the weight of each loss term to 10, 0.5, and 1.5. To determine the ratio of  $\lambda_2$  and  $\lambda_3$ , we statistically analyze the evaluation scores of the results generated under different ratios, as shown in Table 4. As the proportion of  $\lambda_3$  increases, both content loss and LPIPS score increase. Style loss reaches the minimum when the proportion is 0.75. We thus set the ratio to 0.75 for minimizing style loss.

## B. More Results

### B.1. All-to-key Attention VS. All-to-all Attention

To further illustrate the superiority of our proposed all-to-key attention to all-to-all attention in producing high-quality stylized images, we provide more visual comparisons in Figure 10. By replacing all-to-key attention in our full model with all-to-all attention, the visual quality of the stylized images decreases significantly, affected by distorted style patterns.

### B.2. Arbitrary Style Transfer

To further demonstrate the effectiveness and robustness of our proposed StyA2K on arbitrary style transfer, we provide more stylization results of pair-wise combinations between 10 content images and 8 style images (total 80 stylized images) in Figure 11 and Figure 12. Our method can faithfully generate visually appealing results with fine style textures and consistent structures.



---

**Algorithm 1** Pytorch code implementing all-to-key attention.

---

```
1 class A2K(nn.Module):
2     '''All-to-key Attention.'''
3     def __init__(self, in_dim):
4         super().__init__()
5         self.Dq = nn.Conv2d(in_dim, in_dim, (1, 1))
6         self.Dk = nn.Conv2d(in_dim, in_dim, (1, 1))
7         self.Dv = nn.Conv2d(in_dim, in_dim, (1, 1))
8         self.Pq = nn.Conv2d(in_dim, in_dim, (1, 1))
9         self.Pk = nn.Conv2d(in_dim, in_dim, (1, 1))
10        self.Pv = nn.Conv2d(in_dim, in_dim, (1, 1))
11        self.fusion_D = nn.Conv2d(in_dim, in_dim, (1, 1))
12        self.fusion_P = nn.Conv2d(in_dim, in_dim, (1, 1))
13
14    def forward(self, content, style):
15        '''
16        b is batch size; h is the number of heads; c is channel dimension;
17        x is patch sequence length; y is the patch size.
18        H is the feature height; W is the feature weight.
19        Args: content, content feature with shape [b, c, H, W]
20              style, style feature with shape [b, c, H, W]
21        Returns: out, a tensor with shape [b, c, H, W]
22        '''
23        # Get Q K V
24        DA_q = block(self.Dq(mean_variance_norm(Content)), patch_size, stride)
25        DA_k = block(self.Dk(mean_variance_norm(Style)), patch_size, stride)
26        DA_v = block(self.Dv((Style)), patch_size, stride)
27        PA_q = block(self.Pq(mean_variance_norm(Content)), patch_size, stride)
28        PA_k = block(self.Pk(mean_variance_norm(Style)), patch_size, stride)
29        PA_v = block(self.Pv(Style), patch_size, stride)
30        # Distributed Attention
31        logits = torch.einsum("bhcxy,bhcz->bhyxz", DA_q, DA_k)
32        scores = softmax(logits)
33        DA = torch.einsum("bhyxz,bhvzy->bhcxy", scores, DA_v)
34        DA_unblock = unblock(DA)
35        # Progressive Attention Step 1
36        PA1_logits = torch.einsum("bhcxy,bhcz->bhxz", PA_q, PA_k)
37        index = torch.argmax(PA1_logits, dim = -1).expand_as(PA_k)
38        PA_k_reshuffle = torch.gather(PA_k, -2, index)
39        PA_V_reshuffle = torch.gather(PA_v, -2, index)
40        # Progressive Attention Step 2
41        logits2 = torch.einsum("bhcxy,bhcxz->bhxyz", PA_q, PA_k_reshuffle)
42        scores2 = softmax(logits2)
43        PA = torch.einsum("bhxyz,bhcxz->bhcxy", scores2, PA_V_reshuffle)
44        PA_unblock = unblock(PA)
45        # Feature Transformation
46        ODA = self.fusion_D(DA_unblock)
47        OPA = self.fusion_P(PA_unblock)
48        O = ODA + OPA
49        out = O + Content
50        return out
```

---

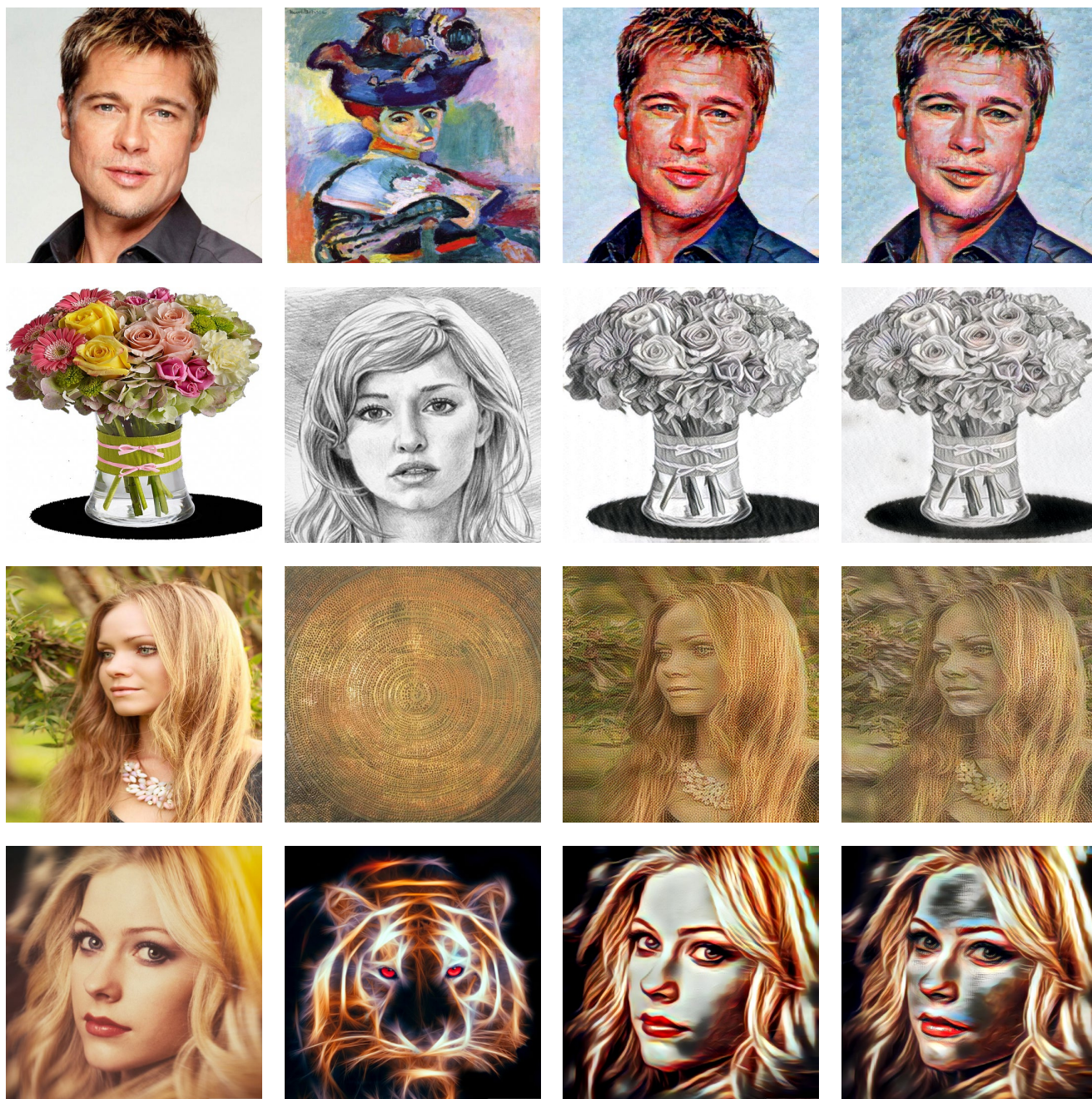
---

**Algorithm 2** Pytorch code implementing feature blocking and unblocking.

---

```
1  def block(X, patch_size, stride):
2      '''feature blocking.
3      Args:
4          X: a tensor with shape [b, c, h, w], where b is batch size, c is the
5             channel dimension, h is feature height, and w is feature width.
6             patch_size: an integer for the patch (block) size
7             stride: the parameter of torch.nn.functional.unfold
8      Returns:
9          Y: a tensor with shape [b, c, n, r], where n is patch sequence length
10             and r is the patch size.
11      '''
12      b, c, h, w = X.shape
13      r = int(patch_size**2)
14      Y = torch.nn.functional.unfold(X, kernel_size=patch_size, stride=stride)
15      Y = Y.view(b, c, r, -1).permute(0, 1, 3, 2)
16      return Y
17
18  def unblock(X, patch_size, stride, h):
19      '''feature unblocking.
20      Args:
21          X: a tensor with shape [b, c, n, r], where b is batch size, c is
22             channel dimension, n is patch sequence length, r is the patch size.
23             patch_size: an integer for the patch (block) size
24             stride: the parameter of torch.nn.functional.unfold
25             h: the output height of the feature
26      Returns:
27          Y: a tensor with shape [b, c, h, w], where h is feature height
28             and w is feature width.
29      '''
30      b, c, n, r = X.shape
31      X = X.permute(0, 2, 1, 3)
32      X = X.contiguous().view(b, n, -1).permute(0, 2, 1)
33      Y = torch.nn.functional.unfold(X, h, kernel_size=patch_size, stride=stride)
34      return Y
```

---



Content

Style

All-to-key Attention

All-to-all Attention

Figure 10. More visual comparisons between our proposed all-to-key attention and all-to-all attention.





Figure 11. More stylization results.





Figure 12. More stylization results.